

# Plastic strain due to twinning in austenitic TWIP steels

B. Qin and H. K. D. H. Bhadeshia\*

Twinning induced plasticity steels are austenitic alloys in which mechanical twinning is a prominent deformation mode, and which exhibit exceptional combinations of ductility, work hardening and ultimate strength. The authors develop in the present paper a crystallographic theory to enable the quantitative investigation of the role of mechanical twinning in enhancing the properties of these alloys. It is found that the twinning strain itself makes a significant though small contribution to the total elongation and that other mechanisms must therefore be at play in determining the overall deformation behaviour.

**Keywords:** TWIP, Twinning, Twinning induced plasticity, Automobiles

## Introduction

Mechanical twinning is a plastic deformation mode that is rarely exploited in engineering applications in the context of steels, largely because the vast majority of practical alloys deform by slip at ordinary strain rates and temperatures. Twinning can, however, form a substantial component of plasticity in steels which are heavily alloyed, for example the Hadfield alloys<sup>1,2</sup> and the modern twinning induced plasticity (TWIP) steels.<sup>3-7</sup>

The TWIP alloys typically contain a large amount of manganese, some aluminium and silicon (e.g. Fe–25Mn–3Si–3Al (wt-%)), and exhibit extraordinary uniform elongation, typically in the range 60–95% (Fig. 1).

Twinning induced plasticity steels are somewhat analogous to transformation induced plasticity (TRIP) steels in which phase transformation enhances plasticity, except that the symmetry of the lattice is preserved by the twinning operation, and the shape deformation due to twinning is a shear strain  $s=1/\sqrt{2}$  which is much larger than the deformation associated with martensitic transformation. The alloys are austenitic and remain so throughout plastic deformation, with the permanent strain being accommodated both via mechanical twinning and slip. The aim of the present work was to examine the contribution of twinning to the overall plastic strain using crystallographic theory alone. Twinning does of course have other effects; the work hardening rate is believed to be enhanced by subdividing the original austenite into twinned and untwinned regions. Although this latter issue is not modelled here, the identification of the contribution of twinning strain to elongation fixes the amount that remains to be

explained in terms of phenomena such as the geometric partitioning of austenite by twins.

## Crystallography

The vector and matrix notation used is due to Bowles and MacKenzie because it is particularly good at avoiding confusion between frames of reference.<sup>8-10</sup> The axes of a polycrystalline sample are defined by an orthonormal set of basis vectors  $[\mathbf{S}; \mathbf{a}_1]$ ,  $[\mathbf{S}; \mathbf{a}_2]$  and  $[\mathbf{S}; \mathbf{a}_3]$ , collectively identified using a basis symbol  $\mathbf{S}$ , where  $\mathbf{a}_i$  are the basis vectors. The crystallographic axes of the  $i$ th austenite grain are similarly identified using the basis symbol  $\gamma_i$  and its corresponding reciprocal basis by the symbol  $\gamma_i^*$ .

Mechanical twinning causes a shear deformation which can be represented by a  $3 \times 3$  deformation matrix  $\mathbf{P}$  such that<sup>8-10</sup>

$$(\gamma \mathbf{P} \gamma) = \mathbf{I} + s[\gamma; \mathbf{d}](\mathbf{p}; \gamma^*) \quad (1)$$

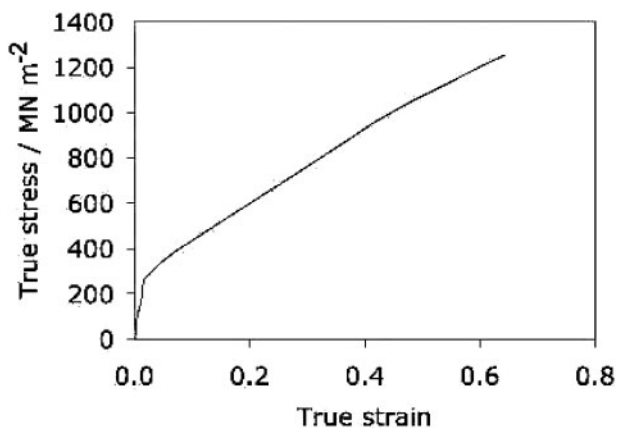
where  $s=1/2^{1/2}$  is the magnitude of the shear,  $[\gamma; \mathbf{d}]$  is a unit vector in the direction of displacement and  $(\mathbf{p}; \gamma^*)$  is the unit normal to the twin plane.

Austenite twins on  $\{111\} \langle 11\bar{2} \rangle$  system, of which there are 12 variants possible in any one austenite grain. Each of these is represented by a crystallographic set, as illustrated below for the first variant listed in Table 1

$$\begin{aligned} \mathbf{p} &|| (1 \quad 1 \quad 1) \\ \mathbf{d} &|| [1 \quad 1 \quad \bar{2}] \\ (\gamma \mathbf{P} \gamma) &= \frac{1}{6} \begin{pmatrix} 7 & 1 & 1 \\ 1 & 7 & 1 \\ \bar{2} & \bar{2} & 4 \end{pmatrix} \\ (\gamma \mathbf{J} \alpha) &= \frac{1}{3} \begin{pmatrix} 1 & \bar{2} & \bar{2} \\ \bar{2} & 1 & \bar{2} \\ \bar{2} & \bar{2} & 1 \end{pmatrix} \end{aligned}$$

Graduate Institute of Ferrous Technology (GIFT), Pohang University of Science and Technology (POSTECH), Pohang 790-784, Republic of Korea

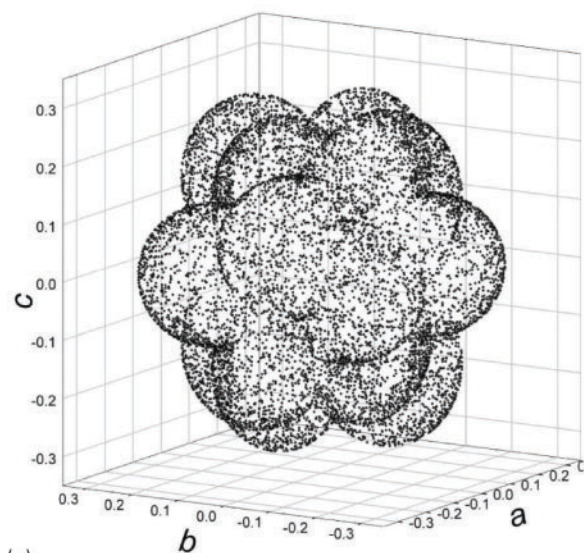
\*Corresponding author, email hkdb@postech.ac.kr



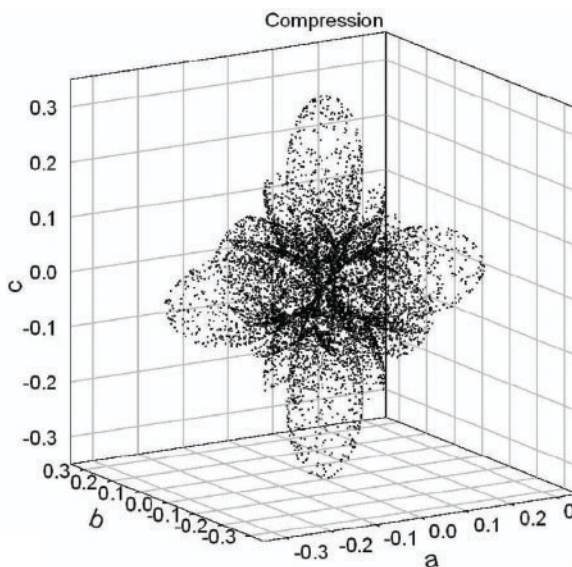
1 Typical stress–strain curve for TWIP steel (courtesy of G. Frommeyer, U. Brück and P. Neumann)

Table 1 The twelve independent mechanical twinning systems in austenite, expressed in the basis  $\gamma$ . The interaction energies listed are calculated for a uniaxial tensile stress of 500 MPa applied to a single crystal along  $[1\ 2\ \bar{7}]_\gamma$

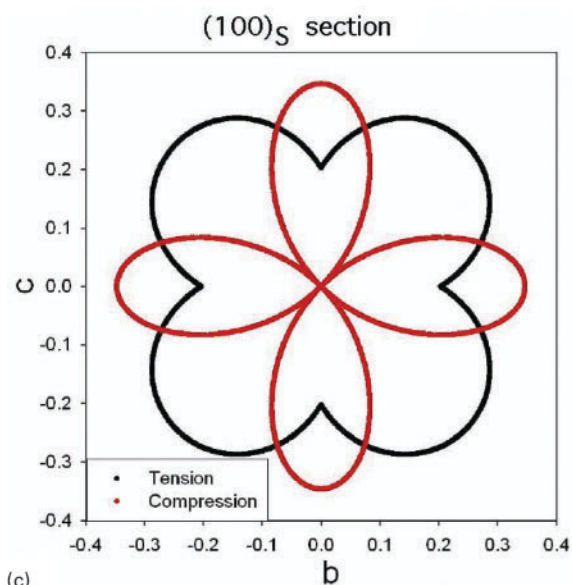
No.	Twin variants	$U, \text{J mol}^{-1}$
1	$(1\ 1\ 1)[1\ 1\ \bar{2}]$	-170
2	$(1\ 1\ 1)[1\ \bar{2}\ 1]$	62
3	$(1\ 1\ 1)[\bar{2}\ 1\ 1]$	108
4	$(1\ \bar{1}\ \bar{1})[1\ \bar{1}\ 2]$	-161
5	$(1\ \bar{1}\ \bar{1})[1\ 2\ \bar{1}]$	25
6	$(1\ \bar{1}\ \bar{1})[\bar{2}\ \bar{1}\ \bar{1}]$	136
7	$(\bar{1}\ 1\ \bar{1})[\bar{1}\ 1\ 2]$	-139
8	$(\bar{1}\ 1\ \bar{1})[\bar{1}\ 2\ \bar{1}]$	111
9	$(\bar{1}\ 1\ \bar{1})[2\ 1\ \bar{1}]$	28
10	$(\bar{1}\ \bar{1}\ 1)[\bar{1}\ \bar{1}\ \bar{2}]$	-105
11	$(\bar{1}\ \bar{1}\ 1)[\bar{1}\ 2\ 1]$	62
12	$(\bar{1}\ \bar{1}\ 1)[2\ \bar{1}\ 1]$	43



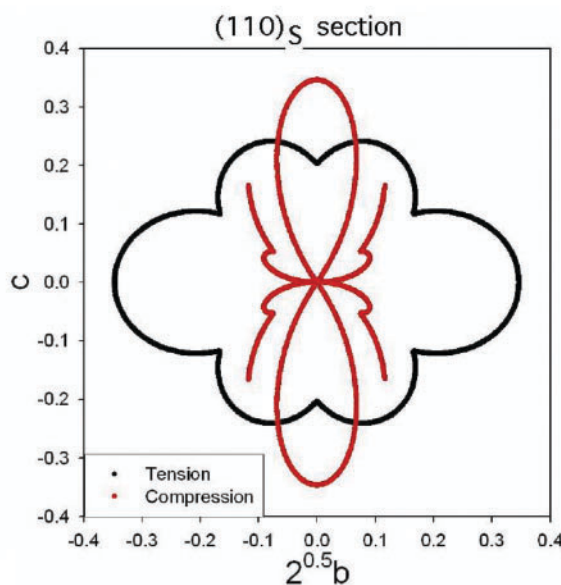
(a)



(b)



(c)



(d)

a uniaxial tension; b uniaxial compression; c section on  $(1\ 0\ 0)$ ; d section on  $(1\ 1\ 0)$

2 Orientation dependence of plastic strain due to twinning of single crystal of austenite (red curves in c and d represent compression)

The method for deriving  $(\gamma J \alpha)$  given the twinning plane and direction is fully described in Ref. 9.

Consider an arbitrary vector  $u$  traversing a grain of austenite before transformation. This vector makes an intercept  $\Delta u$  with a domain of austenite that eventually becomes a twin. As a consequence of the twinning, the vector  $u$  becomes  $v$  given by  $v = P\Delta u + (u - \Delta u)$ . When considering the formation of large numbers of twins in many austenite grains,  $u$  traverses a polycrystalline sample of austenite so this equation must be generalised as follows<sup>11</sup>

$$v = \sum_{k=1}^n \sum_{j=1}^{12} P_j^k \Delta u_j^k + \left( u - \sum_{k=1}^n \sum_{j=1}^{12} \Delta u_j^k \right) \quad (2)$$

where  $j=1\dots 12$  represents the 12 crystallographic variants possible in each austenite grain, and  $k=1\dots n$  represents the  $n$  austenite grains traversed by the vector  $u$ . In this scenario of a large number of twin plates, the intercepts  $\Delta u_j^k$  can be approximated by  $f_j^k u$  where  $f_j^k$  is the fraction of sample transformed by variant  $j$  in austenite grain  $k$ . It can also be demonstrated that over a large number of austenite grains,  $v$  becomes almost parallel to  $u$  so that the true strain due to all the twinning becomes  $\epsilon = \ln\{|v|/|u|\}$ .

The deformation caused by a particular twin  $j$  in austenite grain  $k$ , i.e.  $(\gamma_k P_j \gamma_k) \equiv P_j^k$  can then be expressed in the reference frame of the sample using a similarity transformation as follows<sup>11</sup>

$$(S P_j^k S) = (S R \gamma_k)(\gamma_k P_j \gamma_k)(\gamma_k R S) \quad (3)$$

where  $(S R \gamma_k)$  is the rotation matrix relating the basis vectors of the  $k$ th austenite grain to the sample axes, and  $(\gamma_k R S)$  is the inverse of that rotation matrix. In this way, the calculations can all be referred to the sample frame of reference.

The application of a stress system will favour the formation of particular twin variants which are suitably oriented, i.e. for which the interaction energy  $U$  given by the product of the resolved shear stress  $\tau$  and shear strain is positive.

The applied system of stresses can be described by a  $3 \times 3$  stress tensor  $\sigma_{lm}$  which when multiplied by the unit normal to the twin plane gives the traction  $t$  describing the state of stress on that plane. The traction can then be resolved into  $\tau$  in the normal manner<sup>12</sup>

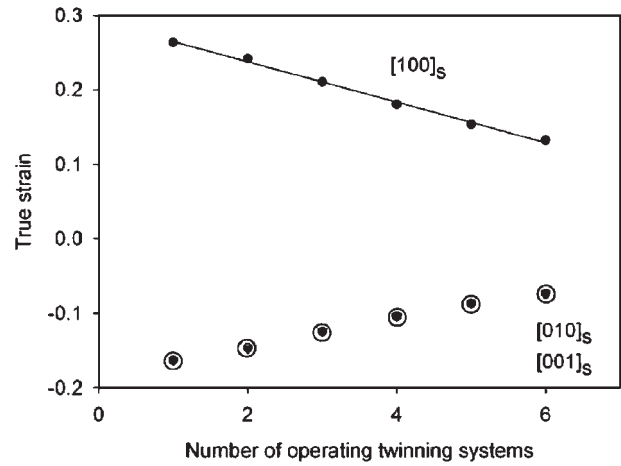
$$\tau = |t| \cos\{\beta\} \cos\{\phi\} \quad (4)$$

where  $|t|$  is the magnitude of  $t$ ,  $\beta$  is the angle between  $t$  and the direction of the maximum resolved shear stress, and  $\phi$  the angle between the latter and the twinning direction. A positive  $U$  means that the strain caused by the twin variant is consistent with the applied stress and vice versa (Table 1).

### Strain surface

Given all the crystallographic characteristics of mechanical twinning and the volume fractions of any twins that form, it is possible to predict the anisotropy of strain when a stress is applied to a single crystal of austenite as a function of the crystallographic orientation of the applied system of stresses.

Figure 2a illustrates how the strain varies with orientation when an entire single crystal of austenite is



3 Predicted strain along sample axes, as function of number of top ranking variants participating in deformation process: sample consists of 10 000 randomly oriented austenite grains which are stressed in tension along  $[1\ 0\ 0]_s$  and which are assumed to be 100% twinned; triangles are for strain along  $[0\ 0\ 1]_s$

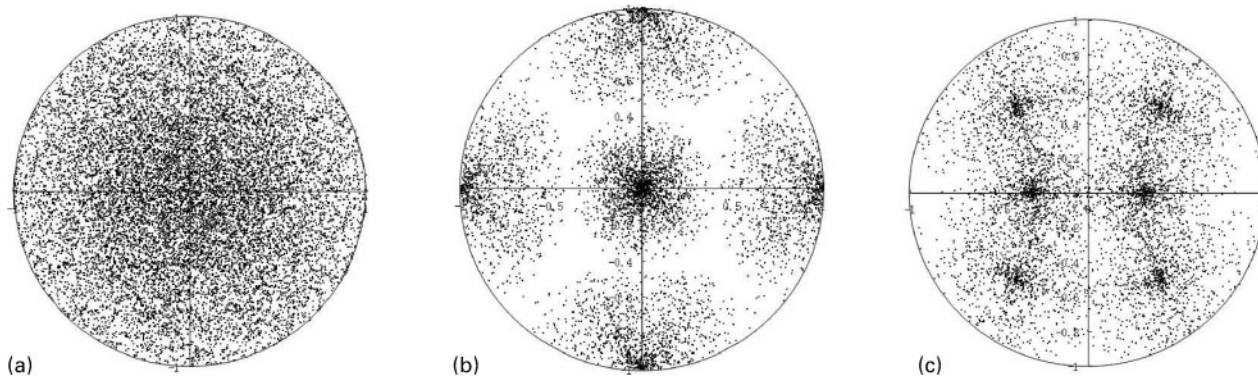
allowed to twin to the most energetically favoured variant, as a function of the orientation of the uniaxial applied tensile stress. The radius at any point corresponds to  $\epsilon$  and the radius vector to the orientation of the tensile axis. It should be pointed out that in some orientations with high symmetry, multiple variants have identical interaction energies; there are 8, 3, 2 and 2 'equivalent' variants for the  $\langle 100 \rangle$ ,  $\langle 111 \rangle$ ,  $\langle 112 \rangle$ ,  $\langle 110 \rangle$  directions respectively, but it is only necessary in each case to consider one system as operating.

There is a huge change in the nature of the strain surface when considering compression (Fig. 2b). It is expected that the strain in uniaxial compression should be large where it is small in uniaxial tension, (Fig. 2c and d). It is, however, surprising that the strain is finite in all tensile directions but is zero during compression along  $\langle 110 \rangle$ . This is because during compression, the  $[110]$  vector is rotated to  $[0.2357\ 0.9428\ 0.2357]$  but is not distorted. Indeed, it has been reported in the literature that the  $\langle 110 \rangle$  direction resists twinning in compression.<sup>13</sup>

It is interesting to examine the characteristic strains in a polycrystalline sample consisting of 10 000 austenite grains randomly oriented relative to the sample axis, under the influence of a tensile stress. To generate a random set of austenite grains, the Euler angles  $\theta_1$  and  $\theta_2$  (ranging from 0 to  $2\pi$ ) and the value of  $\cos \theta$  (between  $\pm 1$ ) are selected using a random number generator.<sup>14</sup> To simulate a polycrystalline state, a number of austenite grains were assembled in this way, each identified by a rotation matrix relating it to the sample frame. The unknowns in the exercise are:

- (i) how many of the variants with a positive  $U$  should be considered
- (ii) how to assign the volume fractions of each of the variants allowed to grow.

Since the only driving force available for twinning is mechanical, it is reasonable to assume that those variants with  $U > 0$  will operate. This is unlike phase transformations where even variants not favoured by the applied stress may form if the chemical driving force is sufficiently large.<sup>15-19</sup> However, the relationship between



a random; b cube; c copper textures

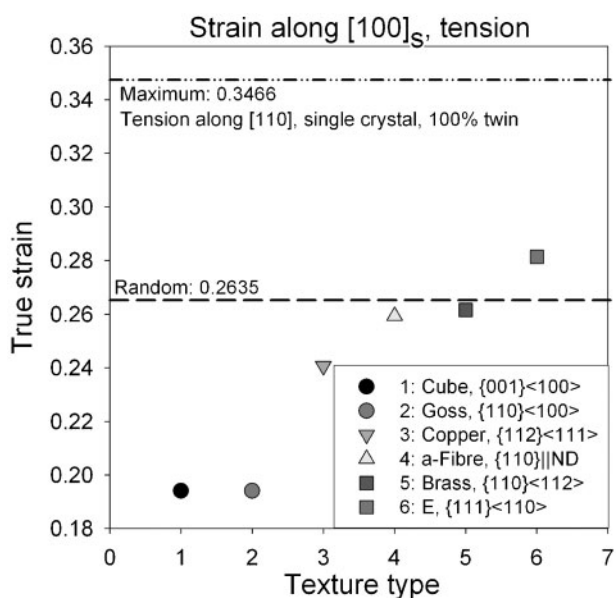
4 Computer generated stereograms showing distribution of  $\langle 1\ 0\ 0 \rangle$  poles: stereograms are centred on  $[0\ 0\ 1]_s$  and vertical direction corresponds to  $[0\ 1\ 0]_s$

$U$  and the volume fraction of a particular twin that can form is not clear. For the present purposes, it is assumed that each austenite grain is equally twinned by each of the variants permitted to grow.

Figure 3 illustrates the three strains along the sample axes, due to twinning. The horizontal axis represents the number of top ranking variants (in terms of  $U$ ) permitted to form per austenite grain. Note also that the interaction energies for these variants will be different for each grain given the distribution of orientations. It is not surprising that the strain along the tensile axis accommodates the applied stress whereas the other two strains along the axes normal to the stress are, as expected, negative. The latter is consistent with the fact that shear does not involve a volume change. The observed strains are clearly sensitive to variant selection, with large changes in both the magnitude and anisotropy of the observed changes.

### Textured austenite

It is possible to generate crystallographically textured austenite before its twinning by placing a limit of the



5 Calculated strain along tensile axis as function of type of texture

rotation angle  $\theta$  allowed in the axis angle pair describing the grain orientation relative to the sample. Some examples of the resulting  $\langle 100 \rangle_\gamma$  pole figures are illustrated in Fig. 4.<sup>20</sup> Extensive calculations have been carried out for a variety of starting textures as illustrated in Figs. 4 and 5. Twin variant selection must depend on the austenite orientation, so it is not surprising that the observed strains are sensitive to texture, and can be greater or less than that expected from a random distribution of austenite grains. Figures 4 and 5 also show the maximum value (0.35) of elongation to be expected if an entire single crystal of austenite is pulled in tension in an optimum orientation.

### Summary

Grassel et al. listed the observed uniform tensile strains in a variety of Fe–Mn–Si–Al austenitic TWIP steels to be in the range 0.45–0.59, values which are much greater than expected from the strain associated with mechanical twinning. The largest plastic strain (0.35) occurs when a single crystal in an optimum orientation becomes completely twinned. The corresponding value for a completely twinned random polycrystal is  $<0.3$  (Fig. 2). The twin fraction is in practice bound to be much less than 1, typically at 0.4 at the point of failure in a tensile test, thus reducing the calculated elongation to  $<0.12$ . Crystallographic texture effects could reduce this further as seen in Figs. 4 and 5.

As pointed out in the introduction, the contribution of mechanical twinning to elongation has been qualitatively understood thus far.<sup>3–7</sup> The present work demonstrates quantitatively that the impressive elongations characteristic of TWIP steels have a rather small contribution from the mechanical strain of twinning, strengthening the case that the increased work hardening attributed to the partitioning of the austenite grains is the major contributing factor to overall elongation. It is interesting that a similar conclusion has been reached in the context of TRIP steels where the martensitic transformation strain makes only a minor direct contribution to the observed plasticity.<sup>21</sup>

### Acknowledgement

The authors are grateful to Professor H.-G. Lee for the provision of laboratory facilities at GIFT, POSTECH and to Dr S. Kundu for helpful discussion.

## References

1. H. C. Choi, T. K. Ha, H. C. Shin and Y. W. Chang: *Scr. Mater.*, 1999, **40**, 1171–1177.
2. I. Karaman, H. Sehitoglu, Y. I. Chumlyakov and H. J. Maier: *J. Met.*, 2002, **54**, 31–37.
3. O. Grassel and G. Frommeyer: *Mater. Sci. Technol.*, 1998, **14**, 1213–1216.
4. O. Bouaziz and N. Guelton: *Mater. Sci. Eng. A*, 2001, **A319–A321**, 246–249.
5. G. Frommeyer, U. Brx and P. Neumann: *ISIJ Int.*, 2003, **43**, 438–446.
6. S. Vercammen, B. Blanpain, B. C. D. Cooman and P. Wollants: *Acta Mater.*, 2004, **52**, 2005–2012.
7. S. Allain, J.-P. Chateau and O. Bouaziz: *Mater. Sci. Eng. A*, 2004, **A387–A389**, 143–147.
8. J. S. Bowles and J. K. MacKenzie: *Acta Metall.*, 1954, **2**, 129–137.
9. H. K. D. H. Bhadeshia: ‘Geometry of crystals’, 2nd edn; 2001, London, Institute of Materials.
10. C. M. Wayman: ‘Introduction to the crystallography of martensitic transformations’; 1964, New York, Macmillan.
11. S. Kundu: ‘Transformation strain and crystallographic texture in steels’, PhD thesis, University of Cambridge, Cambridge, UK, 2007.
12. S. P. Timoshenko and J. N. Goodier: ‘Theory of elasticity’; 1982, London, McGraw Hill International Book Company.
13. P. Yang, Q. Xie, L. Meng, H. Ding and Z. Tang: *Scr. Mater.*, 2006, **55**, 629–631.
14. B. J. Bunge: ‘Mathematische Methoden der Texturanalyse’; 1982, London, Butterworth.
15. A. Matsuzaki, H. K. D. H. Bhadeshia and H. Harada: *Acta Metall. Mater.*, 1994, **42**, 1081–1090.
16. J. W. Stewart, R. C. Thomson and H. K. D. H. Bhadeshia: *J. Mater. Sci.*, 1994, **29**, 6079–6084.
17. S. Kundu and H. K. D. H. Bhadeshia: *Scr. Mater.*, 2006, **55**, 779–781.
18. S. Kundu, K. Hase and H. K. D. H. Bhadeshia: *Proc. Roy. Soc. A*, 2007, **463A**, 2309–2328.
19. S. Kundu and H. K. D. H. Bhadeshia: *Scr. Mater.*, 2007, **57**, 869–872.
20. B. Qin: ‘Crystallography of TWIP steel’, PhD thesis, Pohang University of Science and Technology, Korea, 2007.
21. H. K. D. H. Bhadeshia: *ISIJ Int.*, 2002, **42**, 1059–1060.